

Dynamic response of self-compacting concrete included fiber and eps of hollow beam reinforced with GFRP under impact load

Mohanad T. Abduljaleel ^{*,a}, Abdulkader Ismail Al-Hadithi ^b

Department of Civil Engineering, University of Anbar, Ramadi, Iraq

Article Info

Article History:

Received 12 Oct 2025

Accepted 24 Nov 2025

Keywords:

Plastic fibers;
Impact load;
Inertial force;
Glass fiber reinforced polymer;
Self-compacting concrete

Abstract

The increasing demand for sustainable construction materials has motivated the use of recycled and lightweight constituents in structural concrete. This study investigates the dynamic response of self-compacting concrete (SCC) modified with recycled polyethylene terephthalate (PET) fibers and expanded polystyrene (EPS) beads and reinforced with glass-fiber-reinforced polymer (GFRP) bars. Four reinforced concrete beams (150 × 200 × 1500 mm) were tested under repeated low-velocity impact using a 37.5 kg drop weight released from 3.5 m. Two beams had solid cross-sections, while two incorporated a rectangular internal hollow. Fresh concrete tests confirmed that the modified SCC maintained adequate flowability and cohesion. The average compressive strength was 22 MPa, and density ranged from 1952 to 2301 kg/m³. The dynamic responses were evaluated in terms of displacement, reaction forces, inertial forces, energy absorption, and crack development. The addition of PET fibers increased stiffness and delayed crack propagation, whereas EPS beads reduced density and altered the failure mechanism from brittle to more ductile. Hollow sections increased displacement and inertial forces due to reduced mass and compression-zone depth. Peak displacement during the second impact increased by 2.8–17.3%, and inertial forces rose by up to 66 kN in hollow beams. The combined use of EPS and PET enhanced energy absorption and improved the impact behavior of SCC beams.

© 2025 MIM Research Group. All rights reserved.

1. Introduction

Structural elements in modern infrastructure are often subjected to dynamic and impact loads. Therefore, studies on improving the impact/blast resistance of constructions and civil infrastructure are essential for improving the safety of people from high loads, including missile assaults and explosions. Usually reinforced with continuous deformed steel reinforcing bar (rebar), concrete is vulnerable in tension relative to compression and requires reinforced concrete (RC) construction. The strain rate effect helps the structure to be somewhat resistant against high-speed loads, such as hits and explosions. On the other hand, structural collapse could happen and result in injuries if loads exceed the maximum capability of RC buildings. New materials should thus be developed and used to improve the ultimate load resistance of RC constructions [1]. Incorporating a high volume of discontinuous fiber reinforcements will help to enable the fabrication of high-performance concrete, offering one of the most promising solutions to achieve exceptional impact and blast resistance in concrete and reinforced concrete structures [2].

*Corresponding author: moh22e1001@uoanbar.edu.iq

^aorcid.org/0009-0003-9261-0083; ^borcid.org/0000-0003-2217-7643

DOI: <http://dx.doi.org/10.17515/jresm2025-1241ic1012rs>

Res. Eng. Struct. Mat. Vol. x Iss. x (xxxx) xx-xx

In addition to its energy-absorbing properties, expanded polystyrene (EPS) concrete has excellent resistance to corrosion, water attack, and significant variation in service temperature [3], making it suitable for use in both military and civilian protective constructions [4]. Research on the mechanical reaction of impact-treated EPS concrete is in its early stages, in contrast to that of its quasistatic mechanical properties. Up until now, there has been little reporting on studies examining the dynamic reaction of EPS concrete. One of the most notable uses of lightweight concrete is the engineered materials arrestor system (EMAS). EPS concrete is a strong contender for this role due to its reported dynamic properties, which include a low crushing strength, a large deformation capacity, and good environmental tolerance. A bed constructed at the end of a runway is known as the EMAS. The energy can be dissipated through the crashing of the EMAS material, effectively slowing down the overrunning aircraft. This work presents the results of an initial experimental investigation into the dynamic response of expanded polystyrene (EPS) concrete under low impact velocities, as measured by a drop hammer testing apparatus. Along with the drop hammer testing machine, a high-speed photography system is used to characterize the surface deformation and damage on the EPS concrete during the impact. In light of these findings, the energy dissipation capacity and failure processes of EPS concrete were investigated [5]. Previous studies reported that incorporating crumb rubber (1–2 mm, 5–25% replacement) in steel-fiber concrete decreases compressive strength but significantly enhances impact resistance. Using ACI 544 drop-weight tests on 100×100×500 mm beams, higher crumb-rubber contents consistently increased the measured impact energy despite strength reduction [6].

This study introduces a hybrid SCC incorporating recycled PET fibers, EPS beads, and GFRP reinforcement, a combination not previously examined under repeated low-velocity impact. It further advances the field by assessing engineered hollow sections with central and eccentric voids and by providing millisecond-scale dynamic response data, including reaction, inertia, displacement, and crack evolution. These contributions collectively position the work beyond existing research on EPS-based or fiber-reinforced SCC.

1.1 Research Aim and Objectives

This study aims to examine the influence of recycled PET fibers, EPS lightweight beads, and engineered hollow configurations on the dynamic behavior of self-compacting concrete beams reinforced with GFRP bars under repeated low-velocity impact loading. In pursuit of this aim, the research undertakes the development of modified SCC mixtures incorporating PET fibers and EPS beads, the comparison of solid and hollow beam configurations with identical reinforcement, and the evaluation of displacement histories, reaction forces, inertial responses, and crack propagation during successive impacts. The study further seeks to quantify the combined effects of material modification and section geometry on energy absorption, stiffness characteristics, and overall structural response.

2. Experimental Work

Standard Portland cement (Type I) was used to produce the self-compacting concrete (SCC) mixtures in accordance with ASTM C150 [7]. A highly reactive pozzolanic silica fume (SF), conforming to ASTM C1240, was incorporated as a mineral admixture [8]. The SF contained approximately 85% SiO₂ and had a bulk density of about 700 kg/m³. Superplasticizer (SP), a high-range water-reducing admixture, was employed to achieve the required flowability of SCC. Crushed coarse aggregate with a maximum particle size of 10 mm was used following ASTM C136 and ASTM C33 [9,10]. The fine aggregate was natural river sand with a fineness modulus of 3.7. Spherical expanded polystyrene (EPS) beads were used to partially replace the coarse aggregate, as illustrated in Fig. 1. The EPS beads had an average diameter of 5 mm and a bulk density of 10 kg/m³. Polyethylene terephthalate (PET) waste plastic fibers, with an aspect ratio of 30, were incorporated to enhance the load-carrying capacity and ductility of SCC.

Table 1. Reinforcement rebars properties

Diameter	Type	Yield Strength (MPa)	Ultimate Tensile Strength (MPa)	Elasticity Modulus (GPa)
----------	------	-------------------------	------------------------------------	-----------------------------

6	Steel	570	670	200
10	GFRP	-	1100	45

The properties of the reinforcing bars and waste plastic fibres are presented in Tables 1 and 2, respectively. To produce an environmentally friendly SCC mix with comparable strength, limestone powder was used as a filler material.



Fig. 1. Waste material, (a) Expanded Polystyrene (EPS) and (b) PET fibers

Table 2. Plastic fiber type (PET) properties

Length (mm)	Width (mm)	Thickness (mm)	Aspect ratio	Tensile strength MPa	Elastic Modulus MPa	Specific gravity g/cm ³
33	3	0.3	30	140	1000	1.34

2.1 Specimen Design

The impact performance of (solid-hollow) beams was studied using four concrete beams of 150×200×1500 mm, designed per ACI-440.1R-15 [11]. The specimens were reinforced with two 10 mm GFRP rebars in tension and one 6 mm steel bar in compression. The beam had a 20 mm concrete cover, and for shear force, 6 mm stirrups were positioned at 65 mm apart on the beam. Fig. 2 shows the specimen cross-sectioned. The 120 Ohm strain gauge was attached to the tension bar mid-span and concrete face. Before inserting the strain gauge, the debris was removed by fine sandpaper. All beams have a 0.62% reinforcement ratio.

Two cross-sectional configurations were examined in this study. The solid beams (BR, BS) employed the full 150 × 200 mm section, while the hollow beams (BH1, BH2) incorporated a rectangular void of 50 × 40 mm, corresponding to 6.7% of the total cross-sectional area. In the BH1 specimens, the void was positioned at the neutral axis, whereas in BH2 it was shifted 40 mm downward. This arrangement was adopted to assess how reducing the effective compression-zone depth influences displacement behavior and inertial response under impact loading.

2.2 Impact Load Device

Drop-weight test details are shown in Fig. 3. In the drop-weight test setup, a mechanical mechanism with a clamping system raises a steel hammer to the desired height. Switching the mechanical clamping system releases the steel hammer to produce an impact load. A 45-mm-radius hemispheric steel hammerhead interacts with beams during impact loading. The same hammerhead and impact load were used in all experiments. Impact loads were applied to specimen centers. The 37.5 kg hammerhead was positioned at 3.5 m for all specimens; thus, All beams received approximately 1.3 kJ of impact energy. Piezoelectric accelerometers measured impact loading accelerations in the beam at the L/4 and L/2 of the specimen's span. A displacement transducer (LVDT) positioned at the beam center measured specimen displacements due to impact load. Both supports used dynamic load cells to measure impact loads. National Instruments modules and data acquisition chassis PXI-1042, PXI-4472 recorded and sent specimen impact

loads, displacements, and accelerations to a computer using NI software. The specimens were secured with a thick plate at the beam end to avoid raising; their clear span was 1300 mm. A 1000 FPS camera in front of the specimens was used to monitoring cracks with time. To minimize vibrations, the setup was mounted on a main foundation composed of a heavy steel plate and reinforced concrete. The energy conservation equation was used to calculate energy and velocity: $m = \text{mass}$, $v = \text{velocity}$, $g = \text{normal gravitational acceleration}$, and $h = \text{drop height}$.

$$mgh = 1/2mv^2 \quad (1)$$

$$v = \sqrt{2gh} \quad (2)$$

Due to friction, the mass decreased from rest to beam contact took 0.85 s, adjusting acceleration $a=2h/t^2$ to 9.69 m/s^2 . Equation (1) yields 1270 J without friction, while after applying a new acceleration in equation 1 yielded 1254 J, resulting in a 16 J of energy loss.

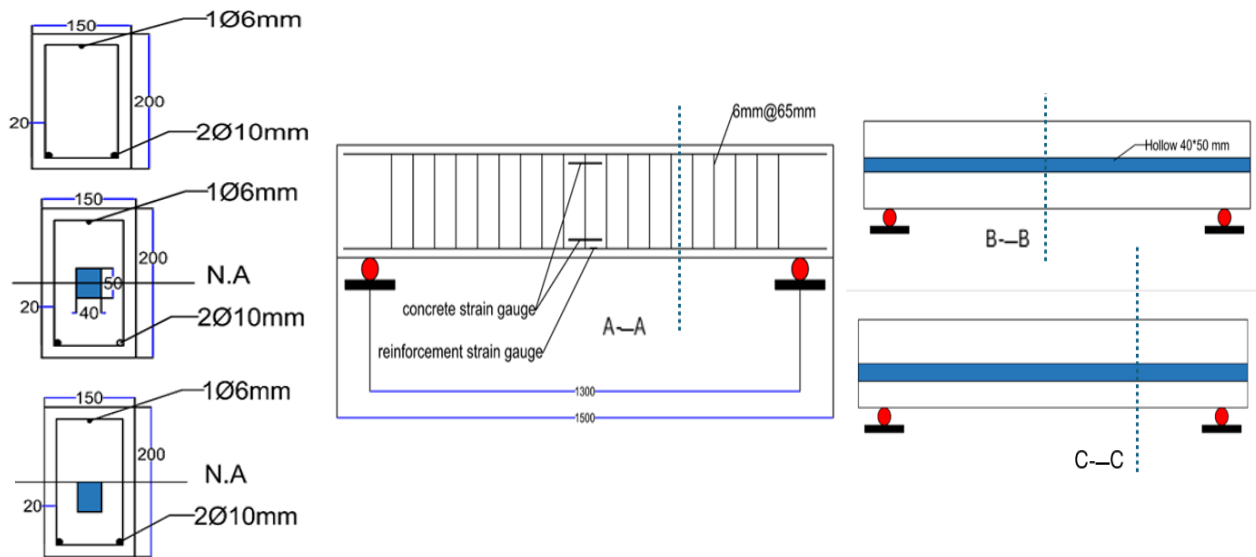


Fig. 2. Demonstrates the reinforcement and hollow location

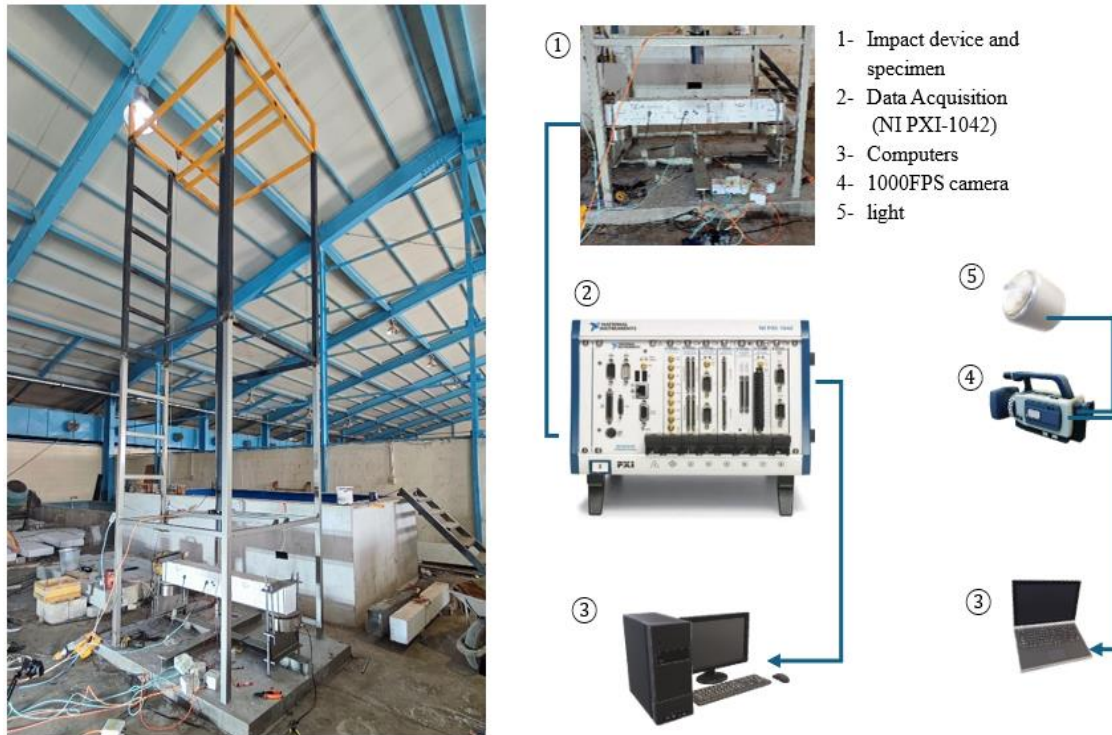


Fig. 3. Details of the impact device and data acquisition

3. Experimental Results and Discussion

3.1 Properties of SCC Contain EPS And Plastic Fiber

Based on fresh characteristics, two materials were chosen, (SR) was the reference material of SCC without fiber and EPS, while (EF) was SCC that contains plastic fiber and EPS beads; Tables 3 and 4 illustrate the trial mix and SCC properties, respectively. The fresh properties test showed that silica-fume (SF) increased matrix cohesiveness [8], prevented the floating of EPS beads, and reduced aggregate segregation. Fresh properties test showed that 2 Kg of EPS beads created SCC correctly according to EFNARC requirements [12]. Incorporating 0.35% PET fibers allowed the SCC to maintain adequate workability while enhancing its mechanical performance. Because EPS beads are weak, cracks started from their surroundings at the ITZ zone, and no compression strength increase was seen over a 90-day period when the compressive strength was tested on 150 mm diameter, 300 mm height cylinders in accordance with ASTM C39 [15]. Although EPS beads cannot carry weights like coarse aggregate, they reduced concrete density by 15 % compared to the reference SR, and accordance to the researcher, curing the EPS surface improves the compressive strength [13]. Two SCC mixes, SR and EF, were tested for compressive strength and density. The average compressive strength was 22.2 MPa, and that was attributed to the use of lightweight EPS as partial replacement from coarse aggregate. This analysis highlights that while strength remained stable, material choice greatly affected the density.

Table 3. Trail mix of SCC

Material* ID	Cement kg/m ³	Fine Agg. kg/m ³	Course Agg. kg/m ³	Water kg/m ³	SF kg/m ³	Fiber (PET) kg/m ³	SP kg/m ³	EPS kg/m ³	Limestone Powder kg/m ³
SR	250	980	700	210	-	-	9	-	230
EF	490	1100	400	189	100	5	13.7	2	-

*SR is a short of self-compacting references (without EPS and fiber), EF refers to the concrete having both (EPS and fiber)

Table 4. SCC mechanical and fresh properties

No.	Material ID	Compressive Strength (MPa)	Tensile strength (MPa)	Density kg/m ³	Slump (mm)	T ₅₀₀ (S)	J-Ring (mm)	V-funnel (S)
1	SR	22.4	2.5	2301	770	2.1	9	9
2	EF	22	3.25	1952	705	3	10	11

3.2 Displacement Response

As shown in Fig. 4 and Table 5, all specimens obtained two impact load first blow and second blows, thus the displacement-time dynamic response may be divided into three stages. Phase 1 saw deflection in the beams from their resting position to their maximum displacement. Phase 2 saw the impact load dropped to zero and the beams returned to their starting point. The beams freely vibrated in Phase 3 after separating from the impactor, similar findings were reported by [14]. Under impact load, all specimens performed somewhat similarly. At second strikes, the displacement values for specimens BR, BS, BH1 and BH2 rose by 2.8%, 10.5%, 17.3%, and 5.3%, respectively. While adding PET fibers increased crack bridging and energy absorption, adding EPS beads in concrete beams reduced stiffness but improved crack separation. The position of the hollow near the middle of the specimen helped BH1 show the most deflection value 12% more than BH2 at second impact load. The presence of a hollow at the center of the specimen reduced the tension and compression zones of the concrete beam, consequently lowering the stiffness value since the compression zone is mostly responsible for the either increasing or decreasing deflection value after reaching the plastic strain in reinforcement rebars. Therefore, it can be concluded that, the displacement of the specimens depends on the depth of the compression zone.

3.3 Force History Response

Separating the inertial loading and total load helps assess impact test results. Brittle materials like concrete have a larger inertial load, or load needed to accelerate the specimen [15]. The beam's bending load is computed by the following equations (3) and (4):

$$P_{t(t)} = P_{b(t)} + P_{i(t)} \quad (3)$$

$$P_{b(t)} = R_{R(t)} + R_{L(t)} \quad (4)$$

The inertial force, total response force of the two supports, and total impact force are denoted as P_i , P_b , and P_t , respectively. The inertial force was computed using the beam's equivalent mass as described in equations (5) and (6).

$$m_{equivalent} = \int_0^L \rho b h \phi(x)^2 dx \quad (5)$$

$$P_{i(t)} = m_{equivalent} \cdot U_{0(t)} \quad (6)$$

In this context, the variables $P_i(t)$ representing the generalized inertial load operating at the beam's center, ρ representing the mass density, $U_{0(t)}$ representing the acceleration at the beam's center, $x = L$ representing the beam's length between supports, and (bh) representing the beam's area are defined. The $m_{equivalent} = \rho b h (L/2)$ for the simply supported beam replace $\phi(x) = \sin(\pi x/L)$. After calculating the total force and inertial force using Eqs. (3) and (6), the experimental results of the total response force are shown in Fig. 5 and Table 5.

Table 5. Impact load experimental result

Beam's name	Material ID	Blow No.	Accumulated energy (kJ)	Midspan displacement Max. (mm)	Reaction force (kN)	*Max. Inertial force (kN)
BR	SR	1	1.2**	14	31	39
		2	2.4	14.41	36.4	
BS	EF	1	1.2	13.68	35.8	50
		2	2.4	15.3	33	
BH1	EF	1	1.2	15.7	31.5	63.9
		2	2.4	19	36	
BH2	EF	1	1.2	15.9	31.19	66
		2	2.4	16.8	31.8	

*The maximum value was selected from Eqs. (3) and (6), **Owing to frictional losses, the impactor's experimentally measured velocity was reduced and limited to about 8 m/s.

The reaction forces during the first blow varied between 31 and 35.8 kN, while during the second blow they ranged from 31.8 to 36.4 kN. The BS specimen, which contained both plastic fiber and EPS beads, showed the highest forces during the first impact load. Specimens BH1 and BR demonstrated a growth of 12.5% and 14.8%, respectively, in the second strike. The redistribution of stress or localized stiffening is probably responsible for the increase in the second impact. Beam responses to impact loads generally followed a similar pattern, these results are consistent with a previous study [16]. At about the same time, the impact force reached a peak on each beam. However, the response force and impact load varied among the beams; this discrepancy may be attributable to the different materials used; for example, the reference material (SR) exhibited the lowest inertial force when contrasted with the changed materials (EF). In line with [1], the use of PET fibers increased the total force of the beam BS by 24% compared to the BR. This is because the fibers improve crack resistance and energy absorption by redistributing stresses through the creation of crack bridges. Consistent with the principles of structural mechanics, the experimental results show that GFRP-reinforced SCC beams with hollow sections have lower stiffness [17,18], and different dynamic behavior under impact. Due to reduced mass and moment of inertia, hollow beams exhibited 11.4-14% lower reaction forces (31 kN vs. 35 kN in solid beams), whereas inertial forces rose (63-66 kN vs. 50 kN), showing enhanced accelerations in lighter and more flexible

systems. The ductility of the SCC matrix was improved by adding EPS beads and 3.5% plastic fibers; this allowed it to delay brittle failure, even in the presence of hollow-induced stress concentrations.

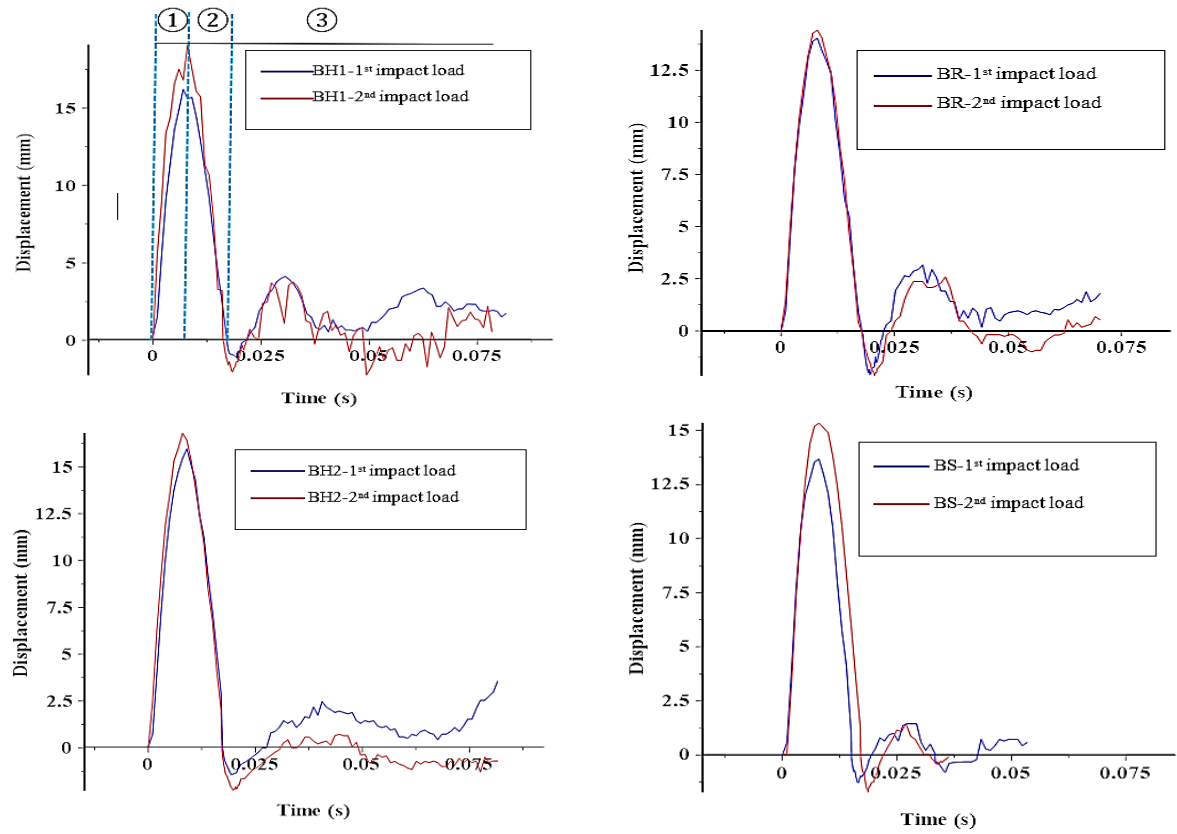
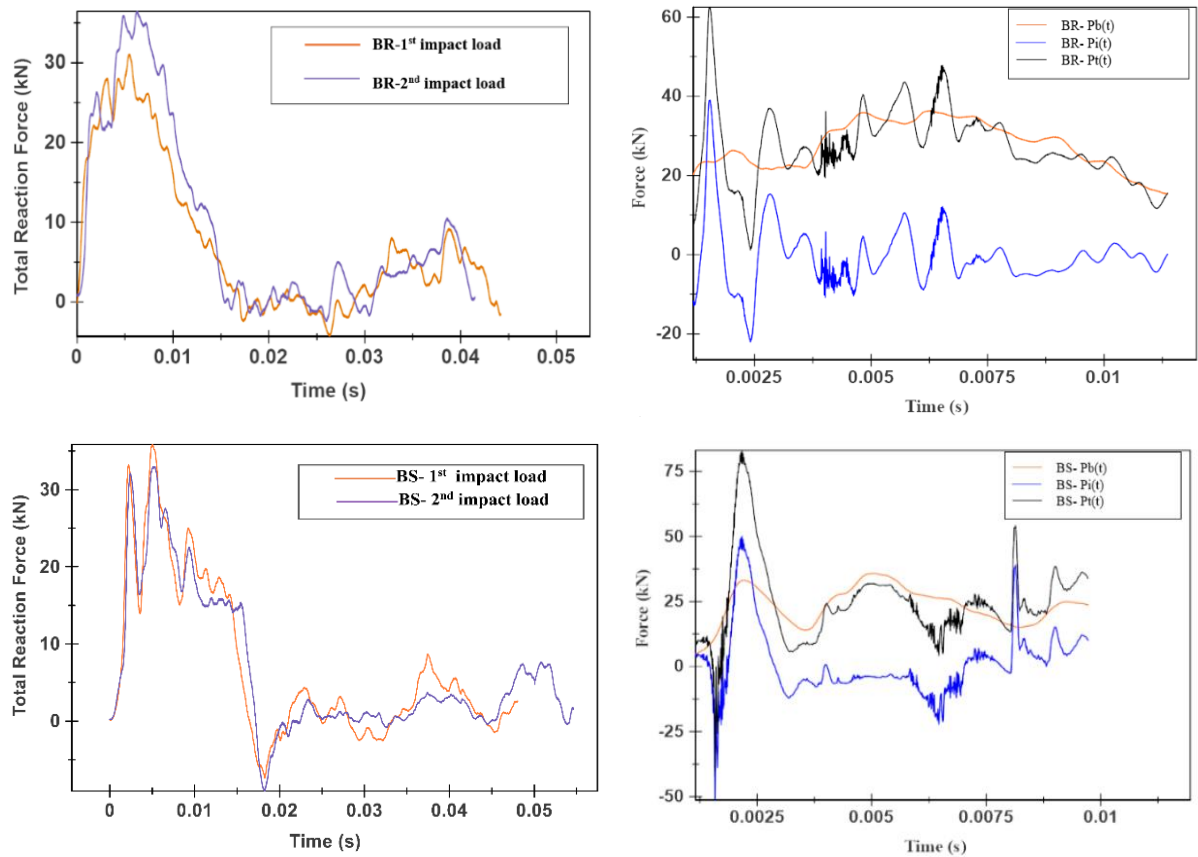


Fig. 4. Displacement response



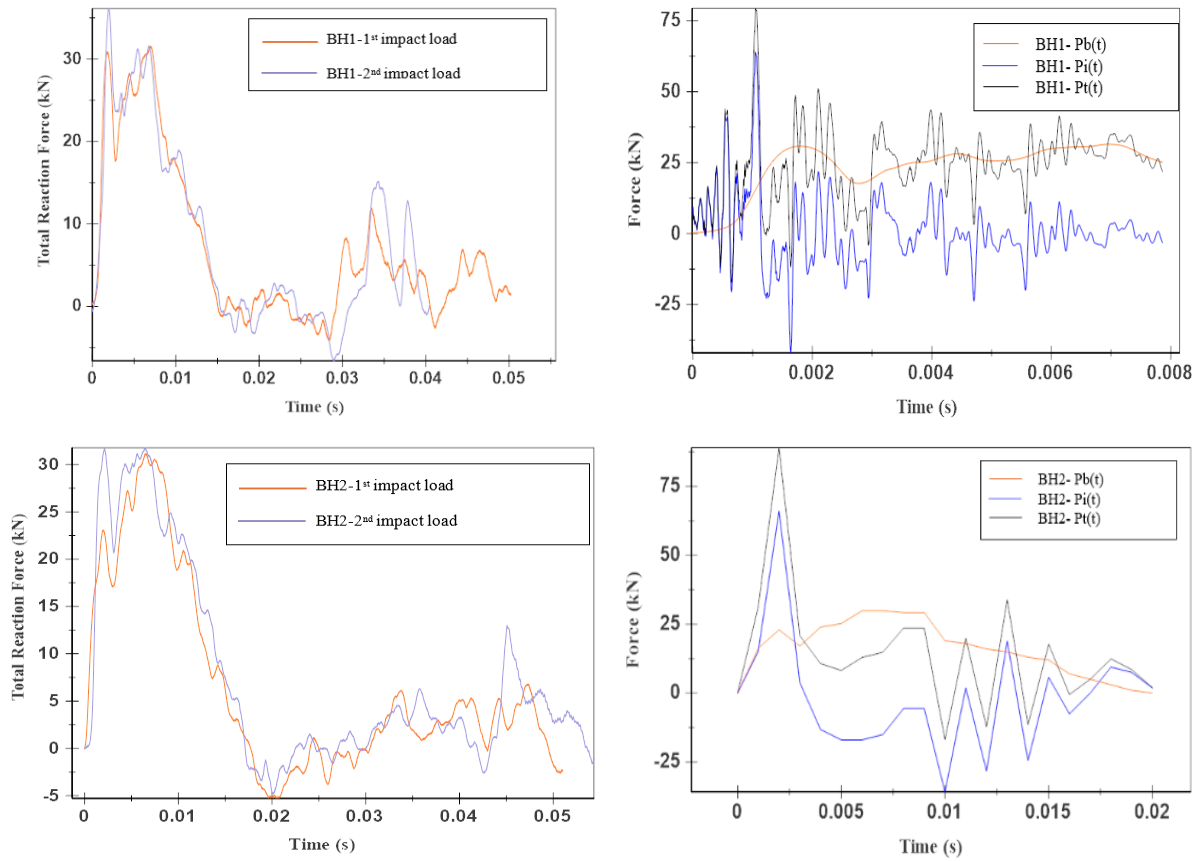


Fig. 5. Time history of reactions and forces

3.4 Cracks and Failure Mode

The same approach has been used to track cracks and failure modes. Four concrete beams were subjected to an impact load, and Figs. 6 and 7 show the cracks developing over time. Each specimen took two strikes from a height of 3.5 meters, and the drop-mass was 37.5 kg. Using a 1000 FPS camera, the crack development in the concrete beams was meticulously tracked. Because of the concentrations of stress, cracks began to form about 2 ms after impact in the area immediately surrounding the tensile zone [13]. Rapid crack propagation along the flexural plane occurred between 7 and 10 ms [19], with crack lengths reaching 160 mm. The specimen BR showed compression failure 25 ms after the second blow, when tensile stresses exceeded the concrete's tensile strength, unlike the specimens with plastic fiber and EPS beads, which demonstrate smooth cracks over time. Different crack patterns were seen in specimens; the hollow beams showed a notable effect on the crack width, resulting in smooth cracks due to the stiffness reduction.

Incorporating expanded polystyrene (EPS) into the concrete mixture improved fracture smoothness and separation when contrasted with the reference beams. According to visual inspection, cracks in the EPS beams were more evenly spaced and less sharp, suggesting better energy dissipation and a more consistent distribution of stress. By reducing stress concentrations and postponing localized failure, the EPS-modified SCC's decreased stiffness probably had a role in this behavior. Because the EPS-modified SCC could not withstand high tensile loads over small areas, its reduced tensile strength led to smoother, more widely spaced cracks. Despite this, the results show that EPS can improve energy absorption and crack management. Unlike the reference beam BR, the behavior of the beams BS, BH1, and BH2 at the second impact load was enhanced and exhibited improvement in the number of load impact cycles, thus incorporating EPS beads with plastic fiber, promising improved resistance to repeated dynamic loads.

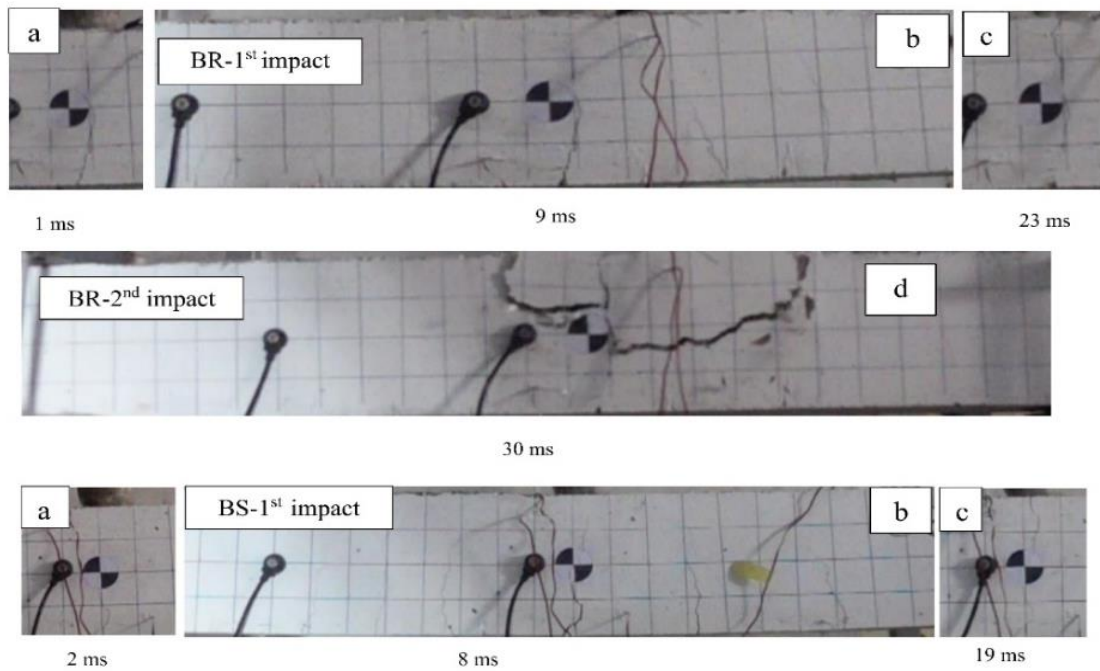


Fig. 6. Failure and crack patterns with time, for BR and BS: (a) first crack; (b) maximum crack distribution; (c) crack at compression zone; (d) maximum crack width at second impact

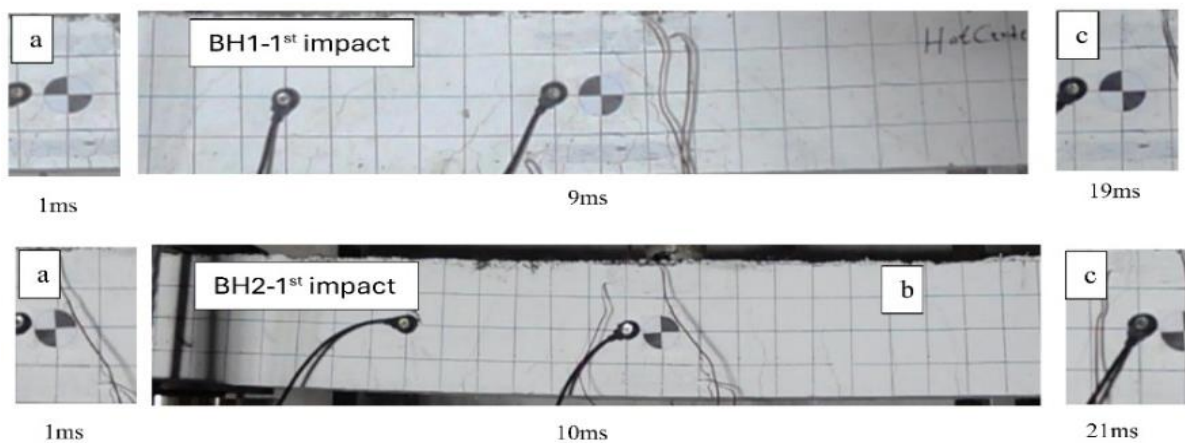


Fig. 7. Failure and crack patterns with time, for BH1 and BH2: (a) first crack; (b) maximum crack distribution; (c) crack at compression zone; (d) maximum crack width at second impact

4. Conclusion

Based on experimental evaluation of SCC beams modified with PET fibers, EPS beads, and hollow sections under repeated impact loading, the following conclusions are drawn:

- The modified SCC achieved an average compressive strength of 22 MPa and density reduction of up to 15% due to EPS inclusion.
- PET fibers improved stiffness and controlled crack propagation, increasing total reaction force by up to 24% compared with reference beams.
- EPS beads changed the failure mode from brittle fracture to smoother, more ductile crack separation.
- Hollow beams recorded 11–14% lower reaction forces but higher inertial forces, caused by reduced mass and stiffness.
- Midspan displacement increased by 2.8–17.3% during the second impact, especially for beams with centrally placed hollows.

- Crack initiation occurred at 1–2 ms after impact and major cracks formed by 8–10 ms, consistent with high-rate loading.
- The combined use of PET and EPS improved energy absorption capacity and repeated-impact resistance.
- Incorporating hollow sections can reduce material consumption while maintaining acceptable dynamic performance.

5. Recommendation

The following points can be considered as recommendations for further research:

- Curing the EPS beads by coating the surface to increase the friction between the cement paste and EPS beads.
- Using a high aspect ratio of around 40 may enhance the load capacity.
- It is recommended to use the EPS as a layer in the tension zone and study the effect.
- Studying the effect of high-speed impact load on the EPS concrete.

Acknowledgment

The writers would like to express their appreciation to the outstanding faculty at the University of Anbar, who generously provided the study with the scientific and technical support it needed.

References

- [1] Chun B, Lee SW, Piao R, Kim S, Yoo DY. Enhanced impact resistance of RC beams using various types of high-performance fiber-reinforced cementitious composites. *Eng Struct.* 2024;319:118790. <https://doi.org/10.1016/j.engstruct.2024.118790>
- [2] Zanuy C, Ulzurrun GS, Curbach M. Experimental determination of sectional forces in impact tests: Application to composite RC-HPFRCC beams. *Eng Struct.* 2022;256:114004. <https://doi.org/10.1016/j.engstruct.2022.114004>
- [3] Perry SH, Bischoff PH, Yamura K. Mix details and material behaviour of polystyrene aggregate concrete. *Mag Concr Res.* 1991;43(154):71-6. <https://doi.org/10.1680/macr.1991.43.154.71>
- [4] Ferrándiz-Mas V, García-Alcocel E. Durability of expanded polystyrene mortars. *Constr Build Mater.* 2013;46:175-82. <https://doi.org/10.1016/j.conbuildmat.2013.04.029>
- [5] Barsotti MA, Puryear JMH, Stevens DJ. Developing improved civil aircraft arresting systems. Vol. 29. Washington (DC): Transportation Research Board; 2009.
- [6] Noamana AT, Abu Bakar BH, Akil HM. Effect of crumb rubber aggregate on toughness and impact energy of steel fiber concrete [doktora tezi]. Penang: Universiti Sains Malaysia; 2016.
- [7] ASTM International. ASTM C150-07: Standard specification for portland cement. West Conshohocken (PA): ASTM International; 2007.
- [8] ASTM International. ASTM C1240-05: Standard specification for silica fume used in cementitious mixtures. West Conshohocken (PA): ASTM International; 2009.
- [9] ASTM International. ASTM C136-06: Test method for sieve analysis of fine and coarse aggregates. West Conshohocken (PA): ASTM International; 2006.
- [10] ASTM International. ASTM C33/C33M: Specification for concrete aggregates. West Conshohocken (PA): ASTM International; 2018.
- [11] ACI Committee 440. ACI 440.1R-15: Guide for the design and construction of structural concrete reinforced with fiber reinforced-polymer (FRP) bars. Farmington Hills (MI): American Concrete Institute; 2015.
- [12] BIBM, CEMBUREAU, ERMCO, EFCA, EFNARC. The European guidelines for self-compacting concrete. Farnham (UK): The Concrete Centre; 2005.
- [13] Zhang L, Huang M, Yang F, Zhang W. A novel hydrophilic modification method of EPS particles: Conception design and performances in concrete. *Cem Concr Compos.* 2023;142:105199. <https://doi.org/10.1016/j.cemconcomp.2023.105199>
- [14] Tran DT, Pham TM, Hao H. Experimental and analytical investigations of prefabricated segmental concrete beams post-tensioned with unbonded steel/FRP tendons subjected to impact loading. *Int J Impact Eng.* 2024;186:104868. <https://doi.org/10.1016/j.ijimpeng.2023.104868>
- [15] Bentur A, Mindess S, Banthia N. The behaviour of concrete under impact loading: Experimental procedures and method of analysis. *Mater Struct.* 1986;19:371-8. <https://doi.org/10.1007/BF02472127>

- [16] Tran DT, Pham TM, Hao H, San Ha N, Vo NH, Chen W. Precast segmental beams made of fibre-reinforced geopolymer concrete and FRP tendons against impact loads. Eng Struct. 2023;295:116862. <https://doi.org/10.1016/j.engstruct.2023.116862>
- [17] Abduljaleel MT, Mahmoud AS, Yousif A. Experiential investigation of two-way concrete slabs with openings reinforced with glass fiber reinforced polymer bars. J Eng Sci Technol. 2017;12(4):898-912.
- [18] Yousif AR, Mahmoud AS, Abduljaleel MT. Punching strength of GFRP reinforced concrete slab-column connections with openings by the finite element method. ZANCO J Pure Appl Sci. 2017;28(6):56-67. <https://doi.org/10.21271/ZJPAS.28.6.8>
- [19] Wei J, Li J, Wu C, Hao H, Liu J. Experimental and numerical study on the impact resistance of ultra-high performance concrete strengthened RC beams. Eng Struct. 2023;277:115474. <https://doi.org/10.1016/j.engstruct.2022.115474>